

**Synthesis and Characterization of Cube-Shaped Cu₂O Nanoparticles
for Heat Transfer Enhancement Application**

by

Mohana Priya A/P Marimuthu

16678

Dissertation submitted in partial fulfilment of

the requirements for the

Bachelor of Engineering (Hons)

(Chemical Engineering)

MAY 2015

Universiti Teknologi PETRONAS

32610 Bandar Seri Iskandar

Perak Darul Ridzuan

CERTIFICATION OF APPROVAL

**Synthesis and Characterization of Cube-Shaped Cu₂O Nanoparticles
for Heat Transfer Enhancement Application**

by

Mohana Priya A/P Marimuthu

16678

A project dissertation submitted to the
Chemical Engineering Programme
Universiti Teknologi PETRONAS
in partial fulfilment of the requirement for the
BACHELOR OF ENGINEERING (Hons)
(CHEMICAL ENGINEERING)

Approved by,

.....
(DR SUJAN CHOWDHURY)

UNIVERSITI TEKNOLOGI PETRONAS

TRONOH, PERAK

MAY 2015

CERTIFICATION OF ORIGINALITY

This is to certify that I am responsible for the work submitted in this project, that the original work is my own except as specified in the references and acknowledgements, and that the original work contained herein have not been undertaken or done by unspecified sources or persons.

(MOHANA PRIYA A/P MARIMUTHU)

ABSTRACT

This project studies on the synthesis of cube-shaped cuprous oxide nanoparticles and evaluation of thermophysical properties of the nanofluid containing synthesized nanoparticles for heat transfer applications. Nanofluids are proven to have higher potential as a cooling medium in heat transfer applications due to its high thermal conductivity property. However, the nanofluids are not stable as the nanoparticles are not well dispersed and forms two layers. Shape of the nanoparticle is also an important factor in ensuring enhanced thermophysical properties of the nanofluid. Hence, in this project, cube-shaped cuprous oxide nanoparticles are synthesized because cube shape has high surface area to volume ratio. A two-step method is chosen as the procedure to prepare the cuprous oxide nanofluid which first focuses on the synthesis of the cuprous oxide nanoparticles in powder form using different bases and continued with the preparation of nanofluid using methanol as the base fluid. The thermophysical properties of the prepared nanofluid is then evaluated to determine the thermal conductivity, viscosity and density.

ACKNOWLEDGEMENT

I would like to express my gratitude to the Chemical Engineering Department of Universiti Teknologi PETRONAS (UTP) beforehand for providing me the Final Year Project (FYP) course as a platform basis to test and sharpen my collective knowledge in Chemical Engineering throughout the five-year study here. Besides that, I would like to thank my FYP supervisor, Dr Sujan Chowdhury, who was always willing to spend his time in assisting and perfecting my project. Through the weekly discussions with my supervisor, I have received numerous shares and insights on the different perspectives for this project to become feasible. His consistent support, patience and effective guidance have brought a great impact to my momentum. Nevertheless, I would also like to thank the FYP coordinator, committees and all lecturers of Universiti Teknologi PETRONAS whom had given me guidance throughout the period of the project. In addition, I would like to take this opportunity to express my deepest gratitude to all relatives which includes my families, kin and friends, and any third party members whom had also contributed both directly or indirectly towards the completion of this project.

TABLE OF CONTENTS

CERTIFICATION OF APPROVAL	i
CERTIFICATION OF ORIGINALITY	ii
ABSTRACT	iii
ACKNOWLEDGEMENT	iv
CHAPTER 1: INTRODUCTION	1
1.1 Background of Study	1
1.2 Problem Statement	3
1.3 Objectives	4
1.4 Scope of Study	5
CHAPTER 2: LITERATURE REVIEW	6
CHAPTER 3: METHODOLOGY	12
3.1 Synthesis of Cuprous Oxide Nanoparticles	12
3.2 Characterization of Synthesized Nanoparticles	13
3.3 Preparation of Nanofluid and Evaluation of Thermophysical Properties	13
3.4 Project Activities	14
3.5 Gantt Chart	16
3.6 Key Milestone	18
CHAPTER 4: RESULTS AND DISCUSSION	19
4.1 Characterization of Cuprous Oxide Nanoparticles	19
4.1.1 TEM Images	19
4.1.2 SEM Images	21
4.1.3 RAMAN Analysis	24
4.2 Evaluation of Thermophysical Properties of Nanofluid	26
4.2.1 Thermal Conductivity of Nanofluid	26

4.2.2 Viscosity of Nanofluid.....	27
4.2.3 Density of Nanofluid.....	29
CHAPTER 5: CONCLUSION AND RECOMMENDATION	31
REFERENCES.....	32
APPENDIX.....	35

LIST OF FIGURES

Figure 2.1	Cube-shaped cuprous oxide nanoparticles	6
Figure 2.2	Copper oxide nanoparticle's size of 200 and 500 nanometers	8
Figure 2.3	Viscosity of copper oxide nanofluid with effect of temperature	10
Figure 2.4	Enhanced thermal conductivity of different copper oxide nanofluids	11
Figure 3.1	The solution's colour change throughout the experiment	12
Figure 3.2	(a) KD2 Prometer, (b) Density meter and (c) Viscometer	14
Figure 3.3	The five divisions under the flow of the project	15
Figure 4.1	TEM images of cuprous oxide nanoparticles prepared using different bases	20
Figure 4.2	FESEM images of cuprous oxide nanoparticles prepared using different bases	22
Figure 4.3	FESEM images of cuprous oxide nanoparticles prepared by sodium bicarbonate at different stirring time	23
Figure 4.4	EDX spectrum indicating the presence of copper and oxygen elements	24
Figure 4.5	Raman spectra of cuprous oxide nanoparticles	25
Figure 4.6	Raman spectra of porous cuprous oxide nanoparticles	25
Figure 4.7	Thermal conductivity of the nanofluid at different temperatures	26
Figure 4.8	Thermal conductivity of the nanofluid at different concentrations	27
Figure 4.9	Viscosity of the nanofluid at different temperatures	28
Figure 4.10	Viscosity of the nanofluid at different concentrations	28
Figure 4.11	Density of the nanofluid at different temperatures	29
Figure 4.12	Density of the nanofluid at different concentrations	30

LIST OF TABLES

Table 1.1 Increase in thermal conductivity of different nanofluid systems	2
Table 1.2 Surface area to volume ratio of different shapes of an object	4
Table 2.1 Thermal conductivity of different nanofluid systems	10
Table 4.1 Weight and atomic percent of copper and oxygen element in the sample	21
Table 4.2 Summary of the cuprous oxide nanofluid's properties	30

CHAPTER 1

INTRODUCTION

1.1 Background of Study

Nanofluids are fluids which is engineered by dispersing nanoparticles in base fluids. In other words, nanofluids are nanoscale colloidal suspensions containing condensed nanomaterials. They are two-phase systems with one phase (solid phase) in another (liquid phase). Some of the common base fluids are water, oil and organic liquids such as ethylene and tri-ethylene glycols.

Nanofluids has been a great interest in heat transfer enhancement applications due to its enhanced thermophysical properties such as thermal conductivity, thermal diffusivity, viscosity, and convective heat transfer coefficients compared to other basefluids like oil or water. It has proven to have potential applications in electronic devices, automotive and heavy duty engines, industrial cooling, building heating systems, nuclear system cooling and cooling system in space station and aircraft. (Yu & Xie, 2012).

Characteristics of nanoparticles such as the material, concentration, size and shape contributes to the nanofluid properties. Materials with the higher thermal conductivity, specific heat, and density are beneficial for heat transfer. Also, the size of nanoparticles defines the surface-to-volume ratio and affects the viscosity of nanofluids. For the same volume concentrations, suspension of smaller particles will have a higher area of the solid/liquid interface. Besides, nanoparticles shapes are strongly related to the total area of the solid/liquid interface. (Timofeeva et al. (2011)). The varied morphology includes nanocubes, nanofibers, nanorods, nanoflowers, nanospheres, octahedral, dendrite-like, eight-horn, honey-comb like, plate-like and many more.

Preparation of nanofluids is the key step in improving the thermal conductivity of fluids. There are two types of methods that have been employed to prepare nanofluids which are single-step method and two-step method. The single-step method is a process combining the preparation of nanoparticles with the synthesis of nanofluids, for which the nanoparticles are directly prepared by physical vapor deposition (PVD) technique or liquid chemical method. In this method the processes of drying, storage, transportation, and dispersion of nanoparticles are avoided, so the agglomeration of nanoparticles is minimized and the stability of fluids is increased. The two-step method for preparing nanofluids is a process by dispersing nanoparticles into base liquids. Nanoparticles used in this method are first produced as a dry powder the nanosized powder is then dispersed into a base fluid in a second processing step. This step-by-step method isolates the preparation of the nanofluids from the preparation of nanoparticles. As a result, agglomeration of nanoparticles may take place in both steps, especially in the process of drying, storage, and transportation of nanoparticles. Simple techniques such as ultrasonic agitation or the addition of surfactants to the fluids are often used to minimize particle aggregation and improve dispersion behavior. (Li et al. (2009)). Table 1.1 shows the increase in thermal conductivity of different nanofluid systems.

TABLE 1.1. Increase in thermal conductivity of different nanofluid systems (Li et al. (2009))

System	Synthesis process	Particle loading (vol%)	Particle size (nm)	Increase in thermal conductivity (%)
Cu/EG	Single-step	0.3	10	40
Cu/H ₂ O	Single-step	0.1	75-100	23.8
Cu/H ₂ O	Two-step	7.5	100	78
Fe/EG	Single-step	0.55	10	18
Ag/toluene	Two-step	0.001	60-80	16.5 (60 °C)
Au/toluene	Two-step	0.00026	10-20	21 (60 °C)
Au/ethanol	Two-step	0.6	4	1.3 ± 0.8
Fe ₃ O ₄ /H ₂ O	Single-step	4	10	38
TiO ₂ /H ₂ O	Two-step	5	15	30-33
Al ₂ O ₃ /H ₂ O	Two-step	5	20	20
Al ₂ O ₃ /EG	Two-step	0.05	60	29
CuO/H ₂ O	Two-step	5	33	11.5
SiC/H ₂ O	Two-step	4.2	25	15.9
NCTs/engine oil	Two-step	2.0	20-50 nm	30
NCTs/poly oil	Two-step	1.0	25 nm × 50 μm	160
NCTs/EG	Two-step	1.0	15 × 30 μm	19.6
NCTs/H ₂ O	Two-step	1.0	15 × 30 μm	7.0
NCTs/decene	Two-step	1.0	15 × 30 μm	12.7
H ₂ O/FC-72	Two-step	12	9.8 nm	52

Whilst, synthesis of nanoparticles involves numerous methods that allows synthesise of various nanostructures with diverse morphologies, sizes, and dimensions using various chemical and physical strategies. Solution-based methods are very common and effective ways to prepare various nanostructures with good control of shape,

composition, and reproducibility. The method have relatively low reaction temperature and suitable for large-scale production. Common solution-based methods are hydrothermal and chemical precipitation techniques. Besides, various nanostructures can be generated through the thermal conversion of the precursors. In this method, the precursors (normally hydroxide or salts like chloride or nitrate) are reacted with alkaline compounds such as sodium hydroxide. However, the thermal dehydration of the precursors, is in solid state involving relatively higher treatment temperature. Next, Electrochemical method is widely used for the preparation of porous nanoparticles. It uses a two-electrode system. Another method to synthesis nanoparticles is thermal oxidation. The process of thermal oxidation involves heat treatment of pure metal substrates in either ambient air or oxygen atmosphere. The morphology of the grown nanoparticles depends on the oxidation temperature, growth time and gas flow rate. (Zhang et al., 2014).





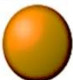
In this project, a nanofluid is prepared through a two-step method which involves the synthesis of cube-shaped nanoparticles and continued by the preparation of nanofluid using water as base fluid. The compound used in this review is cuprous oxide.

1.2 Problem Statement

The surface area to volume ratio is the amount of surface area per unit volume of an object or collection of objects. In chemical reactions involving a solid material, the surface area to volume ratio is an important factor for the reactivity, that is, the rate at which the chemical reaction will proceed. Hence the greater the surface for the same volume, the greater the reactivity. As particles get smaller, their surface area to volume ratio gets larger. With more surface area for the same volume, these small particles react much faster because more surface area provides more reaction sites for the same volume, leading to more chemical reactivity.

Surface area of an object can be calculated by multiplying the number of sides with the length and height of each side. Whilst, the volume of an object can be determined by multiplying the length, width and height. Table 1.2 describes the comparison of surface area to volume ratio for different shapes of an object.

TABLE 1.2. Surface area to volume ratio of different shapes of an object

Shape		Characteristic Length a	Surface Area	Volume	SA/V ratio	SA/V ratio for unit volume
Cube		side	$6a^2$	a^3	$\frac{6}{a}$	6
Octahedron		side	$2\sqrt{3}a^2$	$\frac{1}{3}\sqrt{2}a^3$	$\frac{3\sqrt{6}}{a} \approx \frac{7.348}{a}$	5.72
Dodecahedron		side	$3\sqrt{25 + 10\sqrt{5}}a^2$	$\frac{1}{4}(15 + 7\sqrt{5})a^3$	$\frac{12\sqrt{25 + 10\sqrt{5}}}{(15 + 7\sqrt{5})a} \approx \frac{2.694}{a}$	5.31
Icosahedron		side	$5\sqrt{3}a^2$	$\frac{5}{12}(3 + \sqrt{5})a^3$	$\frac{12\sqrt{3}}{(3 + \sqrt{5})a} \approx \frac{3.970}{a}$	5.148
Sphere		radius	$4\pi a^2$	$\frac{4\pi a^3}{3}$	$\frac{3}{a}$	4.836

Based on the table above, cube shape has surface area to volume ratio of 6 while for sphere shape, the surface area to volume ratio is 4.836. This shows that among the possible shapes, cube shape has the highest surface area to volume ratio for unit volume.

Besides that, stability of the nanofluid is an important factor that influences the properties of nanofluids. The agglomeration of nanoparticles results in settlement and clogging of micro channels hence the thermal conductivity of the nanofluid decreases. This is due to the thermal conductivity of nanofluids depends on the stability and homogeneity of the solution and with the cluster formation. Many methods and techniques for dispersions have been developed to study and analyse the nanofluid to remain homogeneous and stable for a long period, which are sedimentation and centrifugation method, zeta potential analysis and spectral absorbency analysis. There are a few solutions ways to enhance the stability of the nanofluid which includes the use of surfactants or dispersants. This dispersant will increase the contact of two materials or known as wettability. (Yu & Xie, 2012)

1.3 Objectives

The objectives of this project are:

- i. To synthesis cube-shaped cuprous oxide nanoparticles
- ii. To determine the size and morphology of the synthesized cuprous oxide nanoparticles through characterization

- iii. To prepare a stable nanofluid using methanol as base fluid
- iv. To evaluate the thermophysical properties of the nanofluid for heat transfer enhancement application

1.4 Scope of Study

This project focuses on the study of the nanoparticles' synthesis and the prepared nanofluids' thermophysical properties. The synthesis of cube shape cuprous oxide nanoparticles involves chemical reaction of used precursor in alkaline condition. The nanoparticles are characterized through several analysis to determine its size and morphology. Then, the synthesized cuprous oxide nanoparticles are used to prepare the nanofluid using water as base fluid. The final product which is the cuprous oxide nanofluid is evaluated for its thermophysical properties. As a whole, the project involves experimental work throughout the study of the nanofluid's properties for heat transfer applications.

CHAPTER 2

LITERATURE REVIEW

Many researches had been done on the synthesis of different morphologies and sizes of cuprous oxide nanoparticles for various applications. Several methods with different experimental parameters including type of precursors, surfactants and reaction conditions was used to synthesis cuprous oxide nanoparticles. Zhou et al. (2013), Zhao et al. (2008) and Wu et al. (2014) synthesized cube-shaped copper oxide nanoparticles using hydrothermal method. Hydrothermal method involves reaction in a pressurized sealed container and reaction temperature over the critical point of the solution, where the particles are thermally dehydrated to obtain copper oxide nanoparticles. Whilst, Sekhar et al. (2012) used chemical precipitation method which is similar to hydrothermal method but the reaction is conducted in open container with relatively low reaction temperature. Another method is thermal oxidation which was done by Park et al. (2014) for ppb-level formaldehyde gas sensing purpose. There are also new methods were found and applied to synthesis of copper oxide nanoparticles. In that row, Ghosh et al. (2014) synthesized cube-shaped mesoporous copper oxide while Goel et al. (2013) prepared copper oxide micro-cubical structures formation by metal organic chemical vapour deposition.

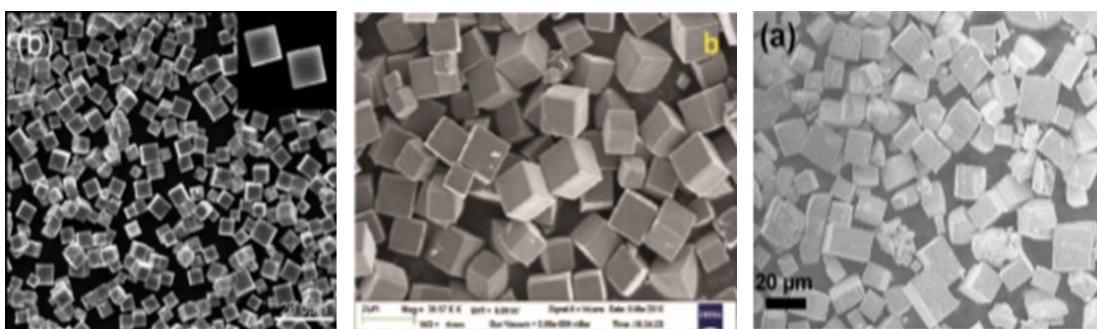


FIGURE 2.1. Cube-shaped cuprous oxide nanoparticles

Precursors are one of the main component in synthesizing copper oxide nanocubes. The concentration and volume of the precursor affects the shape and size of the

nanoparticles. One of the precursor used is copper sulphate (CuSO_4) solution. Basu et al. (2011) used 10 milliliters of 0.01 M CuSO_4 , Sekhar et al. (2012) used 2.5 grams of CuSO_4 , Wu et al. (2014) used 0.45 grams of CuSO_4 , Lin et al. (2014) used 40 milliliters of 0.03 mmol CuSO_4 and Zahmakiran et al. (2009) used 20 milliliters of 1 M CuSO_4 . Another precursor that's used is copper nitrate ($\text{Cu}(\text{NO}_3)_2$) solution. Zhou et al. (2013) used 2.71 grams of $\text{Cu}(\text{NO}_3)_2$ and Zhao et al. (2008) used 30 milliliters of 0.05 M $\text{Cu}(\text{NO}_3)_2$. Besides, many researchers have also shown interest in the use of copper chloride (CuCl_2) solution as a precursor. Hua et al. (2011) and Bao et al. (2010) used 50 milliliters of 0.01 M CuCl_2 , Hu et al. (2012) used 50 milliliters of 0.1 M CuCl_2 and Sharma et al. (2013) used 10 milliliters of 2.93 M CuCl_2 . Besides, copper acetate ($\text{Cu}(\text{CH}_3\text{COO})_2$) solution can also be used as one of the precursors for the synthesis of copper oxide nanoparticles. Cao et al. (2014) used 16.0 milliliters of 0.005 M $\text{Cu}(\text{CH}_3\text{COO})_2$, Zhu et al. (2008) used 300 milliliters of 0.02M $\text{Cu}(\text{CH}_3\text{COO})_2$ and Ma et al. (2010) used 2.3 mmol of $\text{Cu}(\text{CH}_3\text{COO})_2$.

In several studies, the authors had used surfactants as part of their experimental procedure. According to Zhang et al. (2014), surfactants can reduce the interfacial tension between the crystallizing phase and the surrounding solutions, which strongly affects the growth rate and orientation of the crystals. Zhang et al. (2009) and Li et al. (2013) used Polyvinylpyrrolidone (PVP) as a surfactant while Wu et al. (2014) used Sodium dodecyl sulphate (SDS). Next, Ahmed et al. (2011) and Sharma et al. (2013) used Cetyltrimethylammonium bromide (CTAB) as a surfactant.

The size of the copper oxide nanoparticles varies from 30 to 800 nanometers. Park et al. (2014), Zhou et al. (2013), Zhao et al. (2008) and Sekhar et al. (2012) synthesized small range of nanoparticle's size which is below 100 nanomètres. Whilst, in studies conducted by Huang et al. (2008), Li et al. (2013), Ma et al. (2010), Hu et al. (2012) and Lin et al. (2014), the size of nanoparticle ranges from 100 to 500 nanometers. Next, Goel et al. (2013), Basu et al. (2011), Wu et al. (2014) and Sharma et al. (2013) successfully synthesized cube-shaped copper oxide nanoparticle with size ranging from 500 to 800 nanometers.

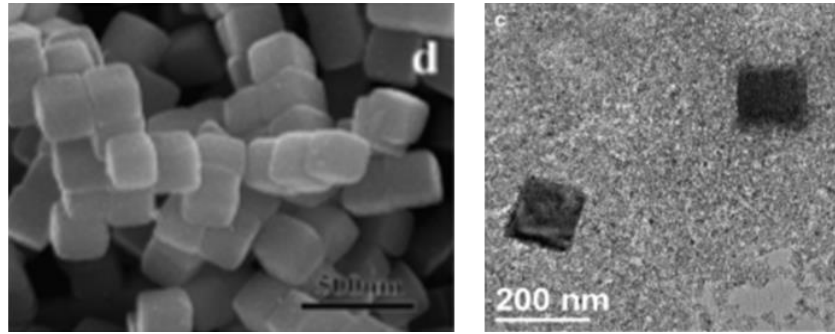


FIGURE 2.2. Copper oxide nanoparticle's size of 200 and 500 nanometers

In addition, preparation of cuprous oxide nanofluids has been a common interest among the researchers. Kumaresan et al. (2014) prepared a stable Cu_2O /Distilled water nanofluid, confirmed through the Zeta potential test. A stability test was conducted by keeping the prepared nanofluid statically for 60 days and no separation line was found between the nanoparticles and water. In Kumaresan et al. (2014) study, the mixture of cuprous oxide and distilled water is kept in an ultrasonic homogenizer at 40 kHz frequency for 60 min duration resulting in uniformly dispersed and good stability. No separation line was found in the nanofluid based on the sedimentation test conducted for 30 days. Besides, Sarafraz et al. (2014) prepared a stable cuprous oxide nanofluid through pH control method and by adding surfactant (sodium dodecyl sulphate (SDS)). The pH value was set at 10.2 while stirring and ultrasonic sonication at 24 kHz were also employed to enhance the stability of nanofluid. At about 1080 hours, the nanofluids were stable without any significant deposition. Sundar et al. (2013) used base fluid of 50:50% volume concentration of ethylene glycol and water. It has shown good stability of cuprous oxide nanofluid that has zeta potential more than 20 mV at pH=1 and 11.

Numerous studies has been carried out for the evaluation of nanofluid's thermophysical properties. The theoretical models that can be used to predict the effective thermal conductivity of the solid–liquid mixture as given below.

- a) Maxwell model for solid–liquid mixtures of relatively large particles (micro-/mini- size) and low solid concentrations.

$$k_{eff} = \frac{k_p + 2k_b + 2(k_p - k_b)\phi}{k_p + 2k_b - (k_p - k_b)\phi} k_b$$

b) Bruggeman model for a binary mixture of homogeneous spherical inclusions.

$$\phi \left(\frac{k_p - k_{eff}}{k_p + 2k_{eff}} \right) + (1 - \phi) \left(\frac{k_b - k_{eff}}{k_b + 2k_{eff}} \right) = 0$$

c) Hamilton and Crosser model for ratio of conductivity of the solid and fluid phases is larger than 100 ($k_p/k_b > 100$)

$$k_{eff} = \frac{k_p + (n - 1)k_b - (n - 1)(k_b - k_p)\phi}{k_p + (n - 1)k_b + (k_b - k_p)\phi} k_b$$

d) Wasp model for special case of Hamilton and Crosser's model with $\psi = 1$

$$K_{nf} = K_{bf} \left[\frac{K_p + 2K_{bf} - 2\phi(K_{bf} - K_p)}{K_p + 2K_{bf} + \phi(K_{bf} - K_p)} \right]$$

In a study conducted by (Kavitha, Rajendran, Durairajan, and Shanmugam (2012)), a summary of measured thermal conductivity of different nanofluid systems has been done, as in below table.

TABLE 2.1. Thermal conductivity of different nanofluid systems

Reference	Base fluid	Nano particle	Size of Nano particle	Maximum Concentration (vol %)	Maximum Enhancement in k (%)
Masuda et al	Water	Al ₂ O ₃	13nm	4.3	30
Eastman et al	Water	Al ₂ O ₃	33nm	5	30
	Water	CuO	36nm	5	60
	Pump oil	Cu	35nm	0.055	45
Pak et al	Water	Al ₂ O ₃	13nm	4.3	32
	Water	TiO ₂	27nm	4.35	10.7
Wang et al	Water	Al ₂ O ₃	28nm	4.5	14
	Ethylene Glycol	Al ₂ O ₃	28nm	8	40
	Pump Oil	Al ₂ O ₃	28nm	7	20
	Engine Oil	Al ₂ O ₃	28nm	7.5	30
	Water	CuO	23nm	10	35
	Ethylene Glycol	CuO	23nm	15	55
Lee et al	Water	Al ₂ O ₃	24.4nm	4.3	10
	Ethylene Glycol	Al ₂ O ₃	24.4nm	5	20
	Water	CuO	18.6nm	4.3	10
	Ethylene Glycol	CuO	18.6nm	4	20
Das et al	Water	Al ₂ O ₃	38nm	4	25
	Water	CuO	28.6nm	4	36
Xie et al	Water	Al ₂ O ₃	60nm	5	20
	Ethylene Glycol	Al ₂ O ₃	60nm	5	30
	Decene	MWCNTs	-	1	20
Liu et al	Synthetic oil	MWCNTs	-	2	30
	Ethylene Glycol	MWCNTs	-	1	12.4

Figure 2.3 and 2.4 shows the experiment conducted by Peyghambarzadeh et al. (2013) where the relationship between viscosity and temperature is determined. The higher the temperature, the lower the viscosity of the copper oxide nanofluid. While, in the experiment by Li et al. (2009), the enhanced thermal conductivity values are determined for different types of copper oxide nanofluid.

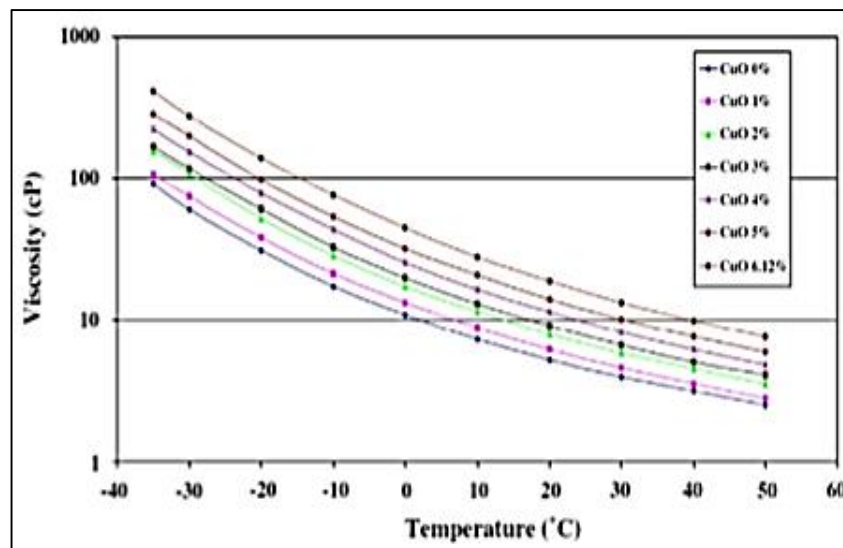


FIGURE 2.3. Viscosity of copper oxide nanofluid with effect of temperature

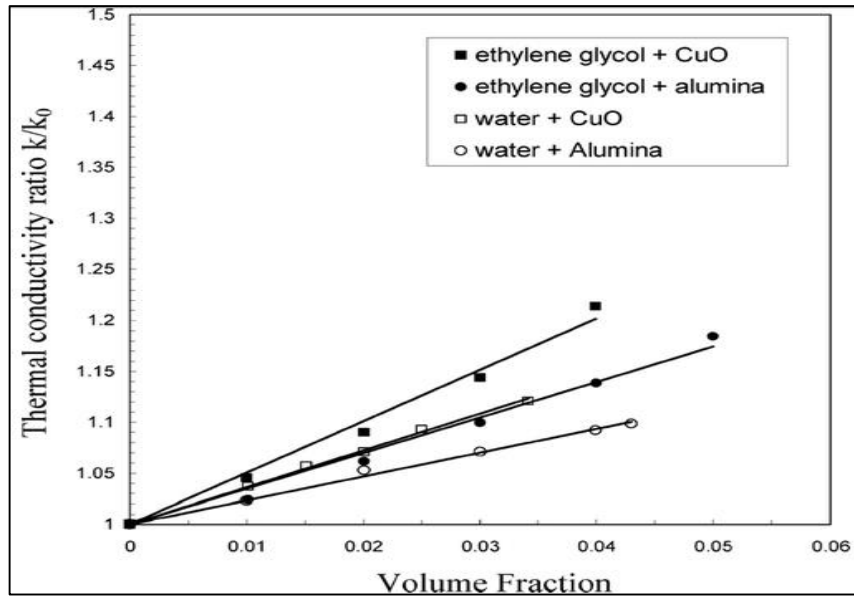


FIGURE 2.4. Enhanced thermal conductivity of different copper oxide nanofluids

CHAPTER 3

METHODOLOGY AND PROJECT WORK

3.1 Synthesis of Cuprous Oxide Nanoparticles

In this project, facile synthesis method was used to produce cube-shaped cuprous oxide nanoparticles. Five different bases were used to synthesis the nanoparticles in order to study the reactivity mechanism while copper chloride (CuCl_2) was used as the precursor and distilled water as the medium. The mentioned bases are sodium hydroxide (NaOH), sodium bicarbonate (NaHCO_3), potassium hydroxide (KOH), ammonium hydroxide (NH_4OH) and ammonium acetate ($\text{C}_2\text{H}_3\text{O}_2\text{NH}_4$). In a typical method, firstly, 10.0 mL of 0.1M CuCl_2 and 30 mL of 0.2M sodium hydroxide (NaOH) were added into 200 mL of distilled water. The solution was left to stir for 10 minutes at room temperature. Following that, 20 mL of 0.1M L-ascorbic acid was added dropwise into the solution and further stirred for two hours under room temperature. The resulting precipitate was centrifuged for 10 minutes under 4000rpm followed by washing with distilled water for several times. Finally, the precipitate was dried in vacuum oven at 50°C for one hour. Figure 3.1 illustrates the colour change of the solution throughout the experiment. The solution was in blue colour when copper chloride and base liquid were added into the distilled water while it turns into pale green once the L-ascorbic acid was added. The solution turns into orange colour in the first hour of experiment and slowly into brown colour in the next hour indicating the formation of cuprous oxide.



FIGURE 3.1. The solution's colour change throughout the experiment

3.2 Characterization of Synthesized Nanoparticles

A number of analysis were conducted to characterize and study on the properties of synthesized cuprous oxide nanoparticles. In order to determine the morphology and size of the nanoparticles, Transmission Electron Microscope (TEM) (Model: Zeiss Libra 200) was used. The products were dispersed into ethanol and kept under ultrasonication for one hour and placed onto a carbon copper grid after 24 hours. The additional structural details were further studied by Selected-Area Electron Diffraction (SAED). Next, images using Variable Pressure Field Emission Scanning Electron Microscope (VPFESEM) (Model: Zeiss Supra55 VP) were taken to further study on the structure of the synthesized nanoparticles. The Raman spectra were collected through a Raman spectrometer (Model: Horiba JobinYvonHR800) to investigate the structural formation of the products.

3.3 Preparation of Nanofluid and Evaluation of Thermophysical Properties

The nanofluid samples were prepared according to the base used to synthesize the cuprous oxide nanoparticles. To prepare the nanofluid, synthesized cuprous oxide nanoparticles were dispersed into the base fluid which is methanol and kept under ultrasonication with 45 kHz frequency for a duration of one hour. A stability test was conducted by keeping the prepared nanofluid statically for 30 days. Two parameters which are temperature and concentration were used to study on the nanofluid's thermophysical properties which includes thermal conductivity, viscosity and density. The temperature was set at 5°C, 10°C, 15°C, 20°C and 25°C while the concentration ranges from 0.05, 0.10, 0.15, 0.30 and 0.50 volume percent (%). The volume concentration of the solution was calculated using below equation.

$$\text{Volume concentration, } \phi = \left(\frac{m_{np}/\rho_{np}}{m_{np}/\rho_{np} + m_{bf}/\rho_{bf}} \right)$$

Figure 3.2(a) shows the measurement of the thermal conductivity of the nanofluid using a KD2 Pro thermal properties analyzer by immersing the probe connected to the device into the nanofluid. While, Figure 3.2(b) shows the measurement of density

evaluated using Mettler Toledo DM40 density meter. The viscosity of the nanofluid was determined using a Brookfield CAP 2000+ viscometer.

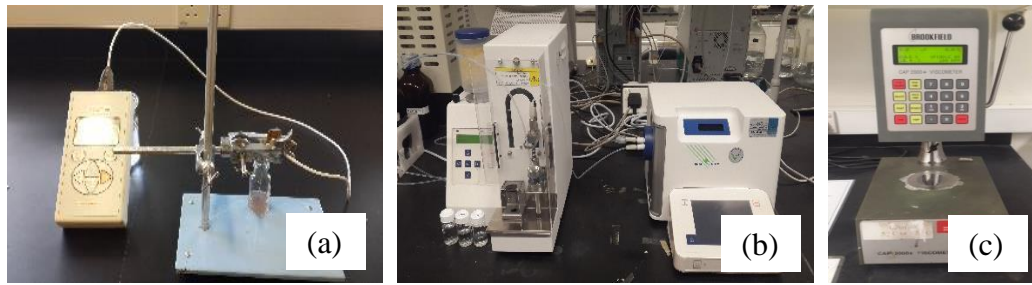


FIGURE 3.2. (a) KD2 Prometer, (b) Density meter and (c) Viscometer

3.4 Project Activities

The flow of the project is divided into five divisions. Figure 3.3 describes the five divisions which starts from the identification of the problem statement and objectives of the project. Following that, a thorough literature review was done and the best methodology and solution was designed. The results and data were collected and analyzed accordingly and proper documentation was completed.

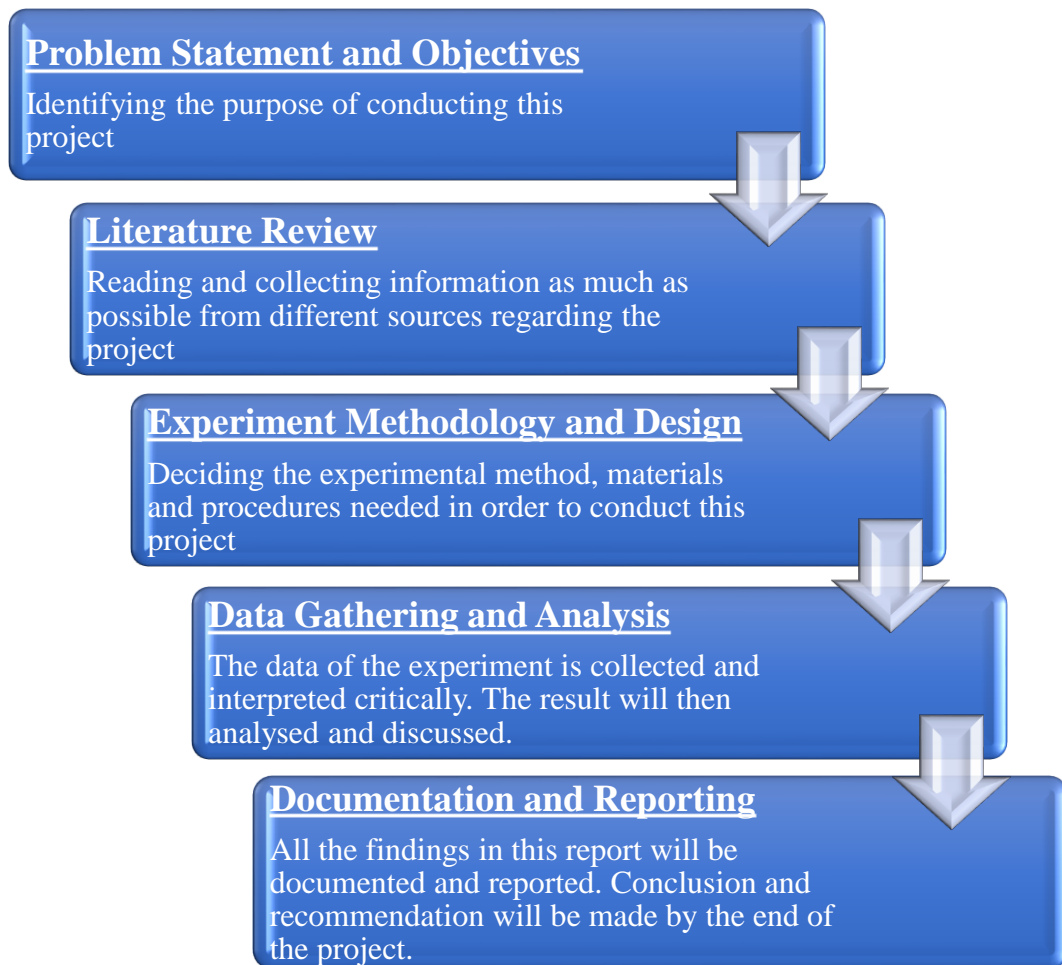


FIGURE 3.3. The five divisions under the flow of the project

3.5 Gantt Chart

ACTIVITIES	WEEKS																											
	FINAL YEAR PROJECT 1														FINAL YEAR PROJECT 2													
	1	2	3	4	5	6	7	8	9	10	11	12	13	14	1	2	3	4	5	6	7	8	9	10	11	12	13	14
Introductory Lecture with The Coordinator	█																											
Selection of Project Title		█																										
First Meeting with Supervisor		█																										
Literature Review			█	█	█	█	█																					
Selection of Model Compound				█	█																							
Selection of Methodology						█	█																					
Preparation and Submission of Extended proposal								◇																				
Preparation of Proposal Defense									█	█																		
Proposal Defense										◇																		
Experimental Work Commences										█	█	█	█	█	█	█	█	█										
Preparation of Interim Draft Report												█																
Completion and Submission of Interim Report													◇															
Sample Testing																		█	█	█	█							
Preparation and Submission																						◇						

3.6 Key Milestone

FYP	Date Start	Date End	Period	Milestones
FYP I	20/1/2015	20/1/2015	1 day	Selected the title for the research project.
	30/1/2015	27/1/2015	4 week	Completed writing the extended proposal report and submitted to the supervisor to be reviewed.
	2/3/2015	4/3/2015	3 days	Made correction to the extended proposal report and submitted to the supervisor to be evaluated.
	3/3/2015	18/3/2015	2 weeks	Completed and presented Proposal Defense.
	11/3/2015	8/4/2015	4 weeks	Completed the interim report writing.
FYP II	18/5/2015	15/6/2015	4 weeks	Completed synthesis of cuprous oxide nanoparticles.
	15/6/2015	6/7/2015	3 weeks	Characterization procedure.
	29/6/2015	27/7/2015	4 weeks	Completed experiment for nanofluid and evaluation of thermophysical properties.
	24/7/2015	21/8/2015	4 weeks	Completed and submission of project dissertation.

CHAPTER 4

RESULTS AND DISCUSSION

The cuprous oxide nanoparticles were synthesized using five different bases at room temperature and stirred for 120 minutes. Characterization of the synthesized nanoparticles were performed using TEM and FESEM while Raman analysis were performed to analyze the structural formation. The thermophysical properties of the nanofluid including thermal conductivity, density and viscosity were measured.

4.1 Characterization of Cuprous Oxide Nanoparticles

4.1.1 TEM Images

Figure 4.1 illustrates the TEM images obtained for all samples of synthesised cuprous oxide nanoparticles. Figure 4.1(a) represents the cube shape of cuprous oxide nanoparticles prepared using sodium hydroxide and the average size of the particles were 62.33 nanometers. While, Figure 4.1(b) and (c) depicts the resultant cuprous oxide nanocages which was prepared using sodium bicarbonate. The white spots on the cubes indicates hollow structure of the nanoparticles with an average size of 819.34 nanometers. Figure 4.1(d) illustrates the cuprous oxide nanoparticles synthesized using potassium hydroxide. The particles have a curvy-edged cube shape and were 78.82 nanometers in size. Next, the TEM image shown in Figure 4.1(e) refers to the cuprous oxide nanoparticles prepared using ammonium hydroxide. The cube shaped nanoparticles have an average size of 59.97 nanometers. The final image which is Figure 4.1(f) illustrates the TEM image of sample prepared using ammonium acetate. The cuprous oxide nanoparticles were in cube shape and 137.80 nanometers in size. It can be concluded that the sample prepared using ammonium hydroxide have the smallest size.

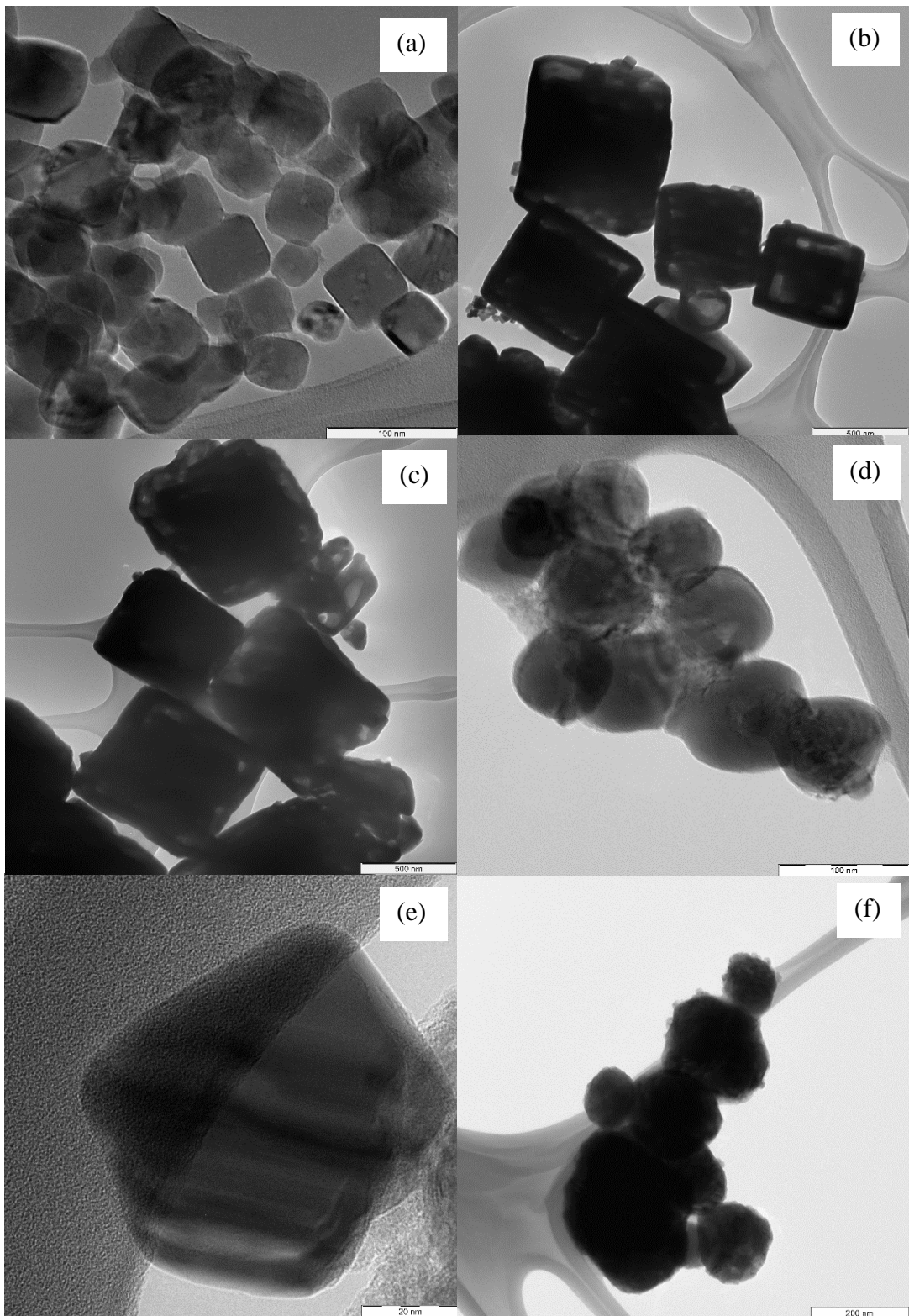


FIGURE 4.1. TEM images of cuprous oxide nanoparticles prepared using different bases

4.1.2 SEM Images

Analysis using Scanning Electron Microscope (SEM) was performed to further analyze the morphology of the synthesized cuprous oxide nanoparticles. Figure 4.2(a) illustrates the cube shaped cuprous oxide nanoparticles prepared using sodium hydroxide. Whereas, Figure 4.2(b) and (c) represents the images of cuprous oxide prepared using sodium bicarbonate. A hollow structure of the cuprous oxide were observed. Figure 4.2(d) and (e) refers to image of cuprous oxide synthesized using potassium hydroxide and ammonium hydroxide respectively. The nanoparticles prepared using ammonium hydroxide have a sharp edged cube shape and were agglomerated. Figure 4.2(f) represents the image of cuprous oxide prepared using ammonium acetate. It can be seen that the particles vary in sizes and some were attached to each other.

As the cuprous oxide nanoparticles prepared using sodium bicarbonate have porous structure, the nucleation and growth process of the hollow structure were studied by varying the stirring time factor. Figure 4.3(a), (b), (c), (d), (e) and (f) shows the FESEM images taken at stirring time of 10, 30, 90, 120, 180 and 300 minutes. At 30th minute, it can be observed that eight cubes of nanoparticles bonds to each other and at 120th minute, the formation of the hollow structure begins from the center of the attached nanoparticles. The porous structure continues to grow and at 180th minute, the particles starts to split into smaller particles until the 300th minute.

Energy Dispersive X-Ray (EDX) analysis were performed to determine the components in the samples prepared. Table 4.1 represents the weight and atomic percent of the copper and oxygen elements present in the samples prepared. While, Figure 4.4 describes the spectrum obtained from the analysis indicating the presence of copper and oxygen element in the samples.

TABLE 4.1. Weight and atomic percent of copper and oxygen element in the sample

Element	Weight%	Atomic%
O	19.16	48.49
Cu	80.84	51.51
Total	100.00	

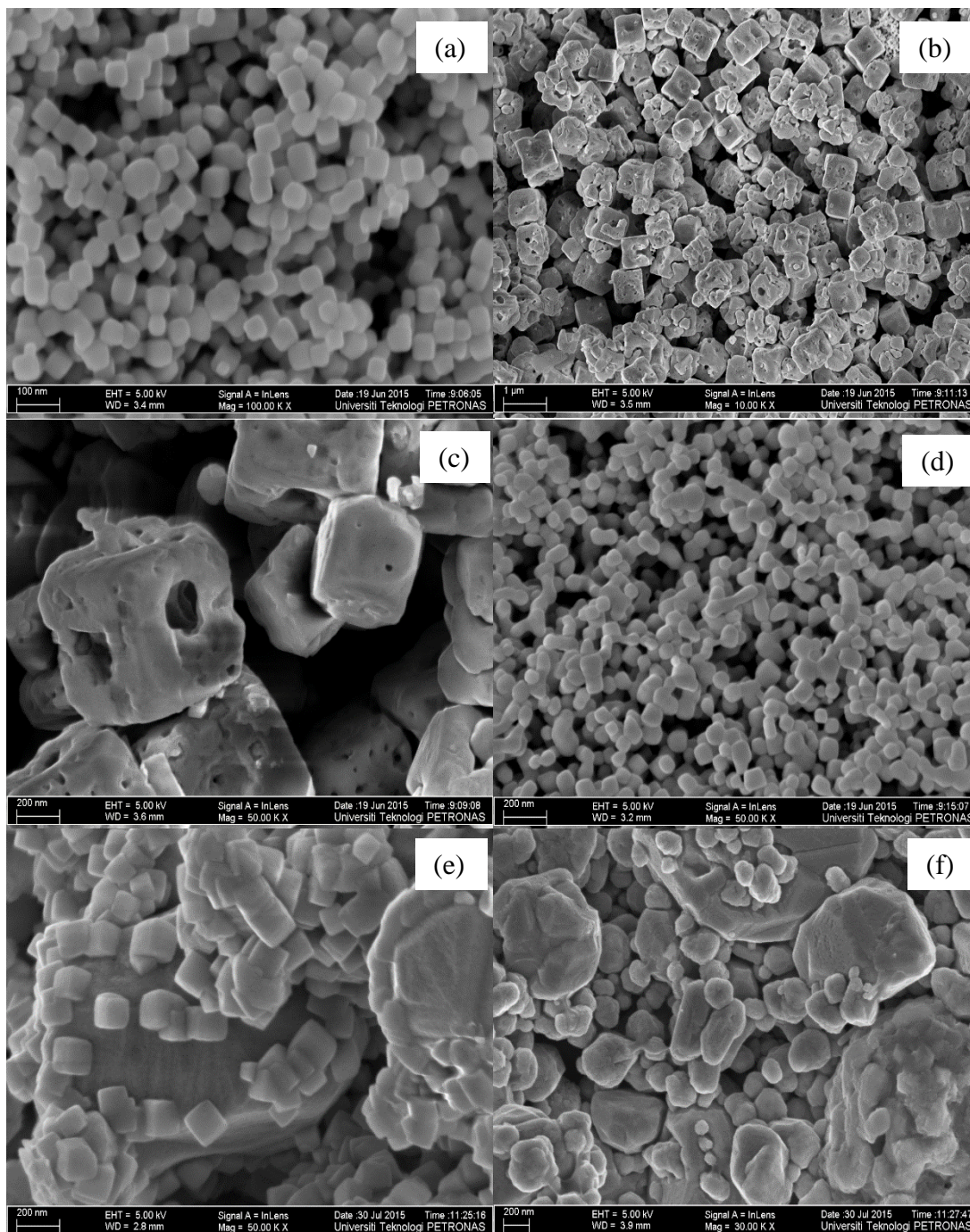


FIGURE 4.2. FESEM images of cuprous oxide nanoparticles prepared using different bases

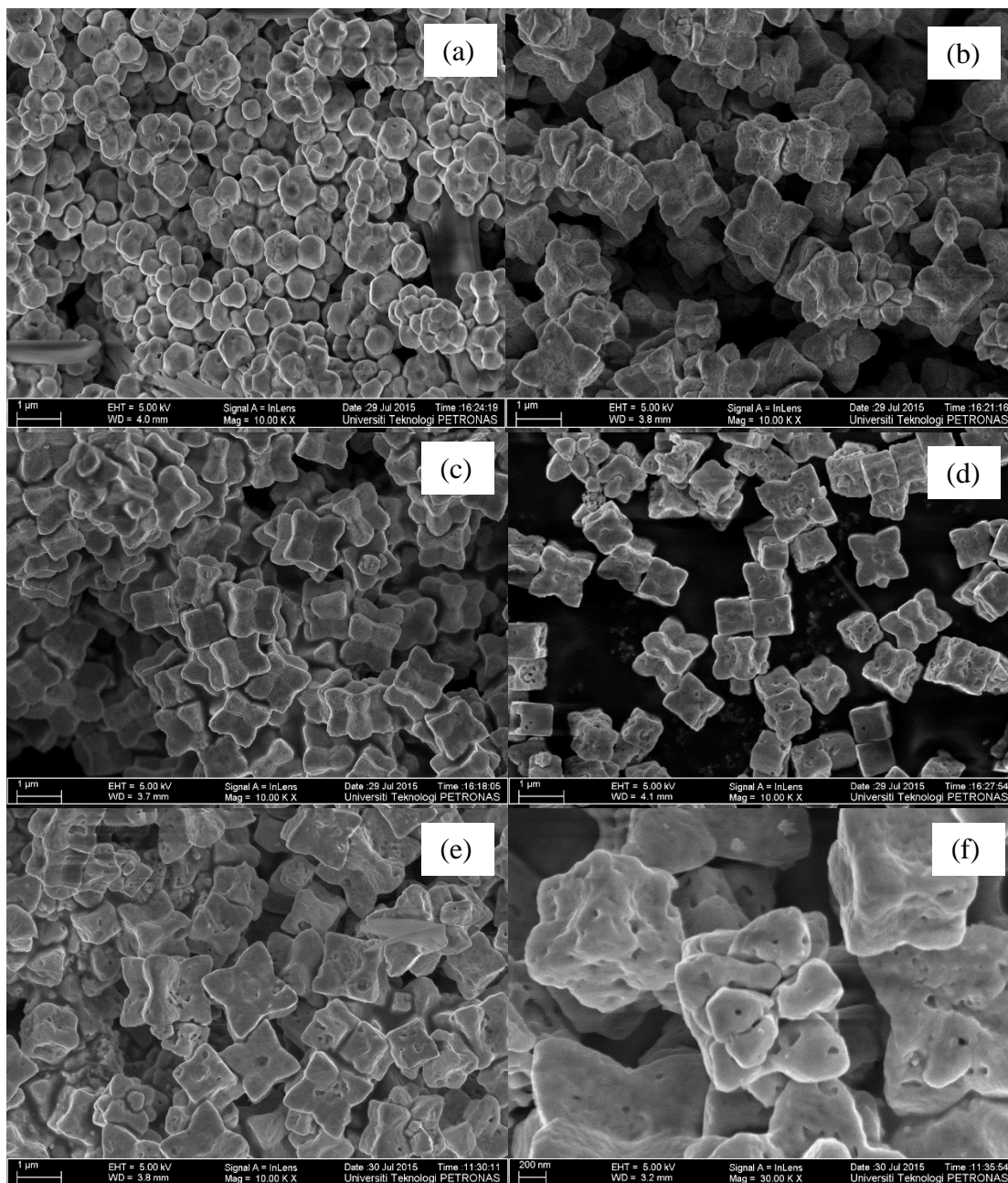


FIGURE 4.3. FESEM images of cuprous oxide nanoparticles prepared by sodium bicarbonate at different stirring time

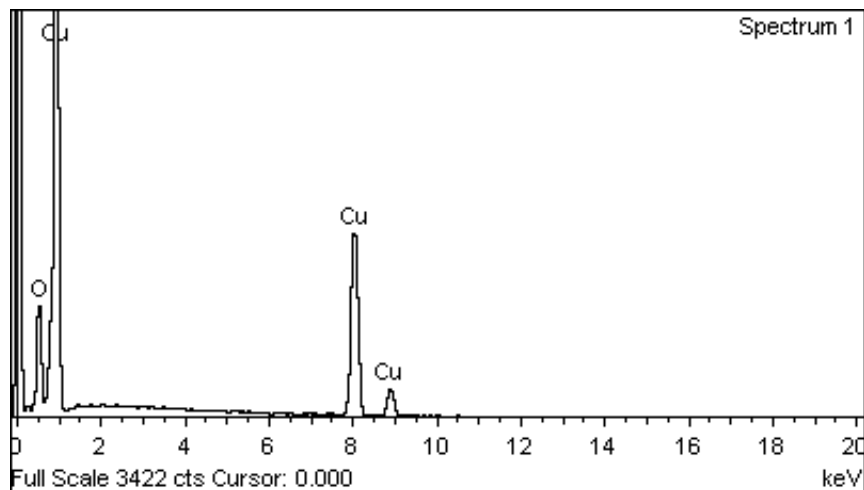


FIGURE 4.4. EDX spectrum indicating the presence of copper and oxygen elements

4.1.3 RAMAN Analysis

The structural formation of the cuprous oxide nanoparticles were studied by Raman scattering. Figure 4.5 shows the Raman spectrum of the cuprous oxide nanoparticles. The Raman spectrums of the samples describe the characteristic phonon frequencies of the crystalline cuprous oxide. The strong peak at 209 cm^{-1} originated from the second-order Raman-allowed mode of the cuprous oxide crystals. The peak at 128 cm^{-1} is assigned to the inactive Raman mode. While, the peak at 172 cm^{-1} may be attributed to Raman scattering from phonons of symmetry. The weak peak at 409 cm^{-1} correspond to the second-order overtone. The peak at 615 cm^{-1} is attributed to the infrared-allowed mode. The characteristic peaks of CuO under the same experimental conditions at 330 and 602 cm^{-1} could not be detected. Hence, all samples contain pure cuprous oxide without copper oxide impurities.

Figure 4.6 represents the Raman spectrums for the hollow structured cuprous oxide nanoparticles. Comparing both spectrums, strong peaks can be observed at 180th minutes of stirring indicating the presence of cuprous oxide particles.

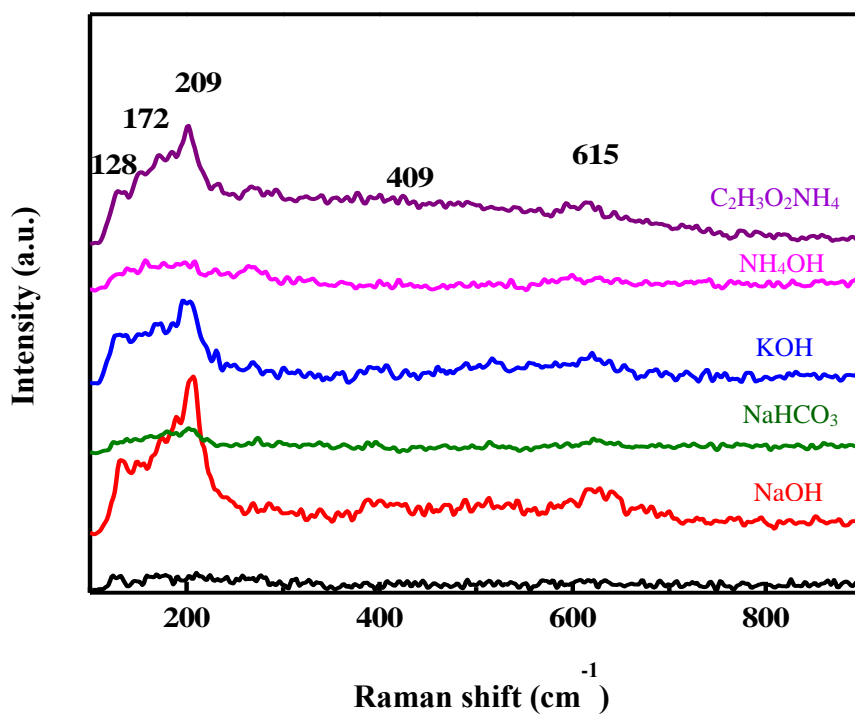


FIGURE 4.5. Raman spectra of cuprous oxide nanoparticles

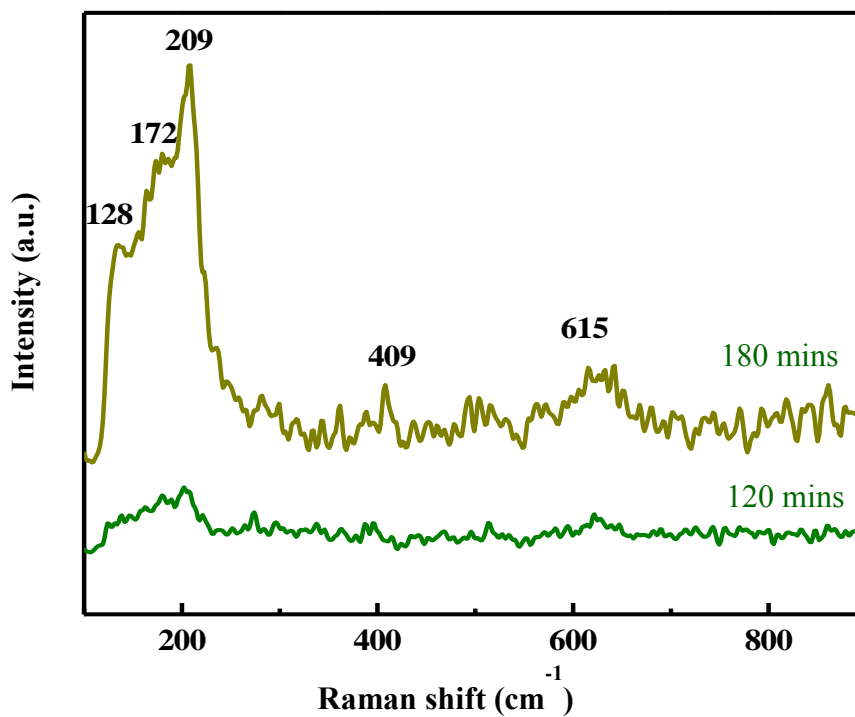


FIGURE 4.6. Raman spectra of porous cuprous oxide nanoparticles

4.2 Evaluation of Thermophysical Properties of Nanofluid

4.2.1 Thermal Conductivity of Nanofluid

The thermal conductivity of the nanofluid were measured for each sample using KD2 Pro thermal analyzer for two parameters which are temperature and concentration. Figure 4.7 represents the thermal conductivity for different temperatures. As the temperature increases, the thermal conductivity of all samples increases too. Among them, cuprous oxide nanofluid which was prepared using potassium hydroxide yields the highest thermal conductivity which is 0.1305 W/m.K at 25°C. While, Figure 4.8 shows the thermal conductivity values at different temperatures. It is observed that as the concentration increases, the thermal conductivity of the nanofluid increases as well. The experimental values were compared with the values obtained from the reference, Nader et al. (2014). The experimental thermal conductivity values are higher at low concentration compared to the reference values. The highest value obtained is 1.306 W/m.K at 0.5 volume percent.

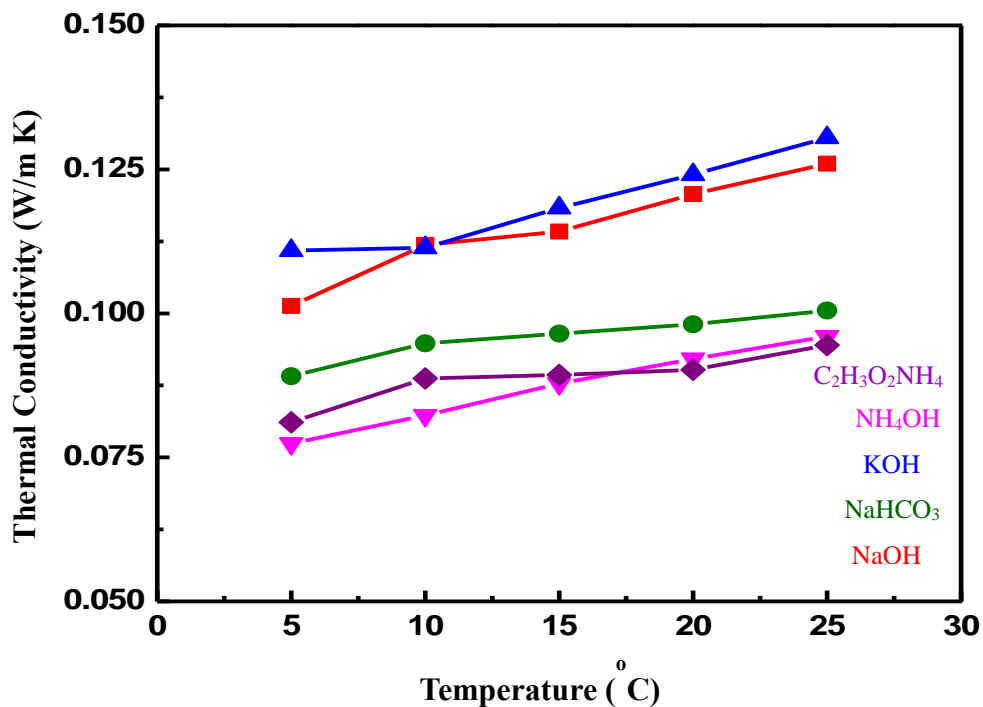


FIGURE 4.7. Thermal conductivity of the nanofluid at different temperatures

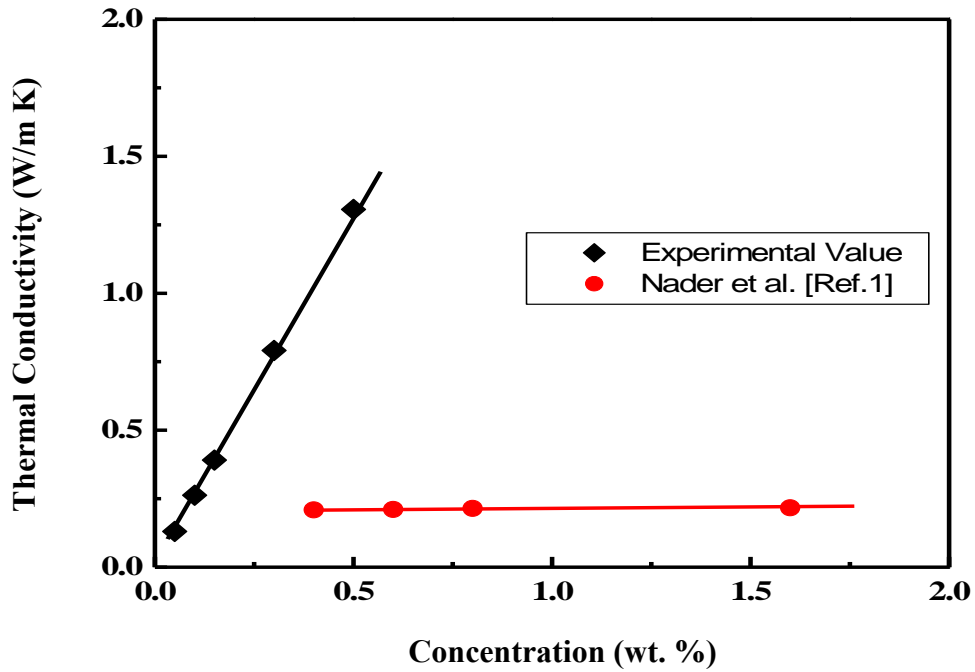


FIGURE 4.8. Thermal conductivity of the nanofluid at different concentrations

4.2.2 Viscosity of Nanofluid

The viscosity of the nanofluid are measured using a viscometer at different temperatures and concentrations. Figure 4.9 shows the viscosity of the nanofluid at different temperatures. As the temperature increases, the viscosity of the nanofluid decreases. Cuprous oxide nanofluid prepared by ammonium acetate has the lowest viscosity which is 559.3 centiPoise at 25 °C. However, in Figure 4.10 which represents the viscosity of nanofluid at different concentrations, shows that the viscosity increases as the concentrations increases. Comparing the experimental values with the values obtained from the reference, it is observed that the experimental viscosity values are higher at low concentration compared to the reference values.

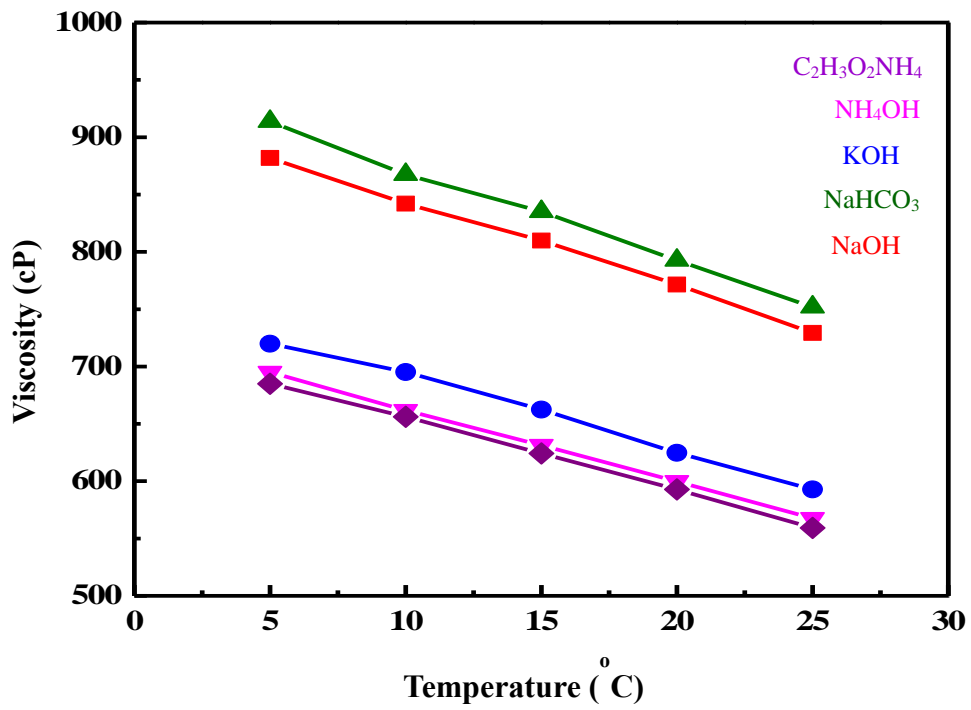


FIGURE 4.9. Viscosity of the nanofluid at different temperatures

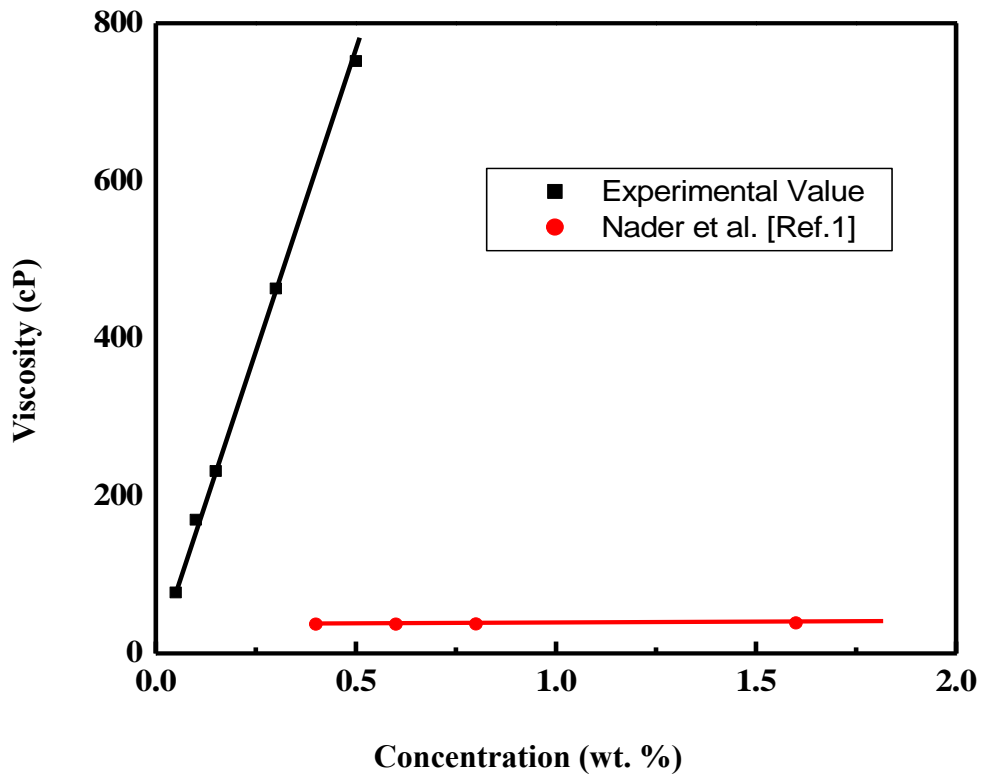


FIGURE 4.10. Viscosity of the nanofluid at different concentrations

4.2.3 Density of Nanofluid

The density of the nanofluid are measured using a density meter at different temperatures and concentrations. Figure 4.12 shows the density of the nanofluid at different temperatures. As the temperature increases, the density of the nanofluid decreases. Cuprous oxide nanofluid prepared by ammonium acetate has the lowest density which is 0.079 g/cm^3 at 25°C . Whereas, in Figure 4.12 which represents the density of nanofluid at different concentrations, shows that the density increases as the concentrations increases due to its increasing mass of nanoparticles in the nanofluid.

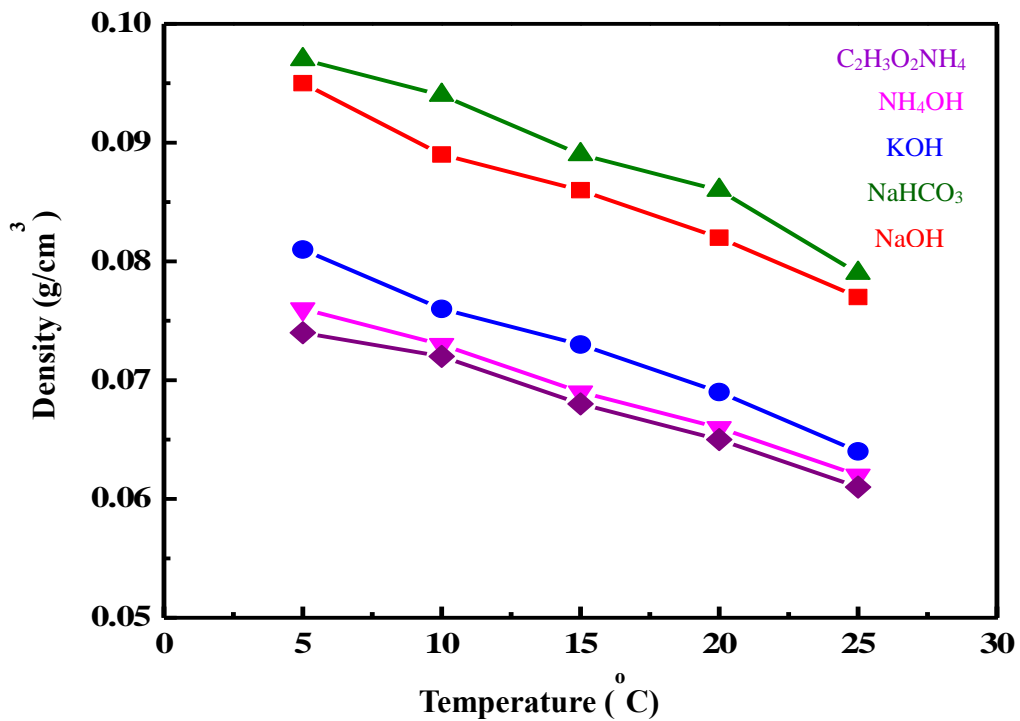


FIGURE 4.11. Density of the nanofluid at different temperatures

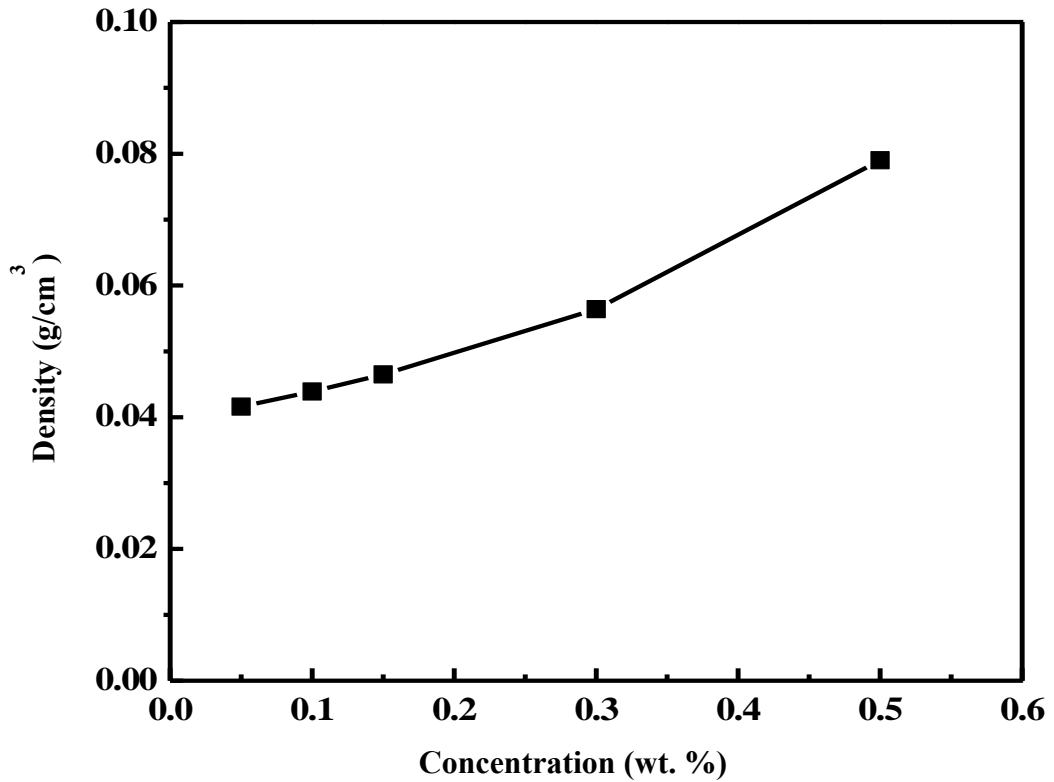


FIGURE 4.12. Density of the nanofluid at different concentrations

The nanofluids prepared using different bases have different thermophysical properties including the thermal conductivity, viscosity and density. Table 4.2 summarizes the properties of the synthesized cuprous oxide nanoparticles and its thermophysical properties.

TABLE 4.2. Summary of the cuprous oxide nanofluid's properties

Sample	Average Particle Size (nm)	Thermal conductivity (W/m.K)	Viscosity (cP)	Density (g/cm ³)
NaOH	62.33	0.1260	729.3	0.077
NaHCO ₃	819.34	0.1005	592.8	0.064
KOH	78.82	0.1305	751.9	0.079
NH ₄ OH	59.97	0.0960	567.6	0.062
C ₂ H ₃ O ₂ NH ₄	137.80	0.0945	559.3	0.061

CHAPTER 5

CONCLUSION AND RECOMMENDATION

The objective of this project is to synthesize cube-shaped cuprous oxide nanoparticles and to prepare a stable nanofluid which has enhanced thermophysical properties. A two-step method was used where the cuprous oxide nanoparticles were synthesized using five different bases and copper chloride as a precursor followed by the preparation of cuprous oxide nanofluid using methanol as base fluid. Several analysis were performed to analyze the size and morphology of the nanoparticles which includes TEM, FESEM and Raman. TEM images depicts the cube shaped cuprous oxide nanoparticles which sizes ranging from 59.97 – 819.34 nanometer. The sample prepared using ammonium hydroxide gives the smallest size of nanoparticles while sample prepared using sodium bicarbonate gives porous structures of cuprous oxide. Using the synthesized nanoparticles, nanofluid were prepared under ultrasonication. The thermophysical properties which are thermal conductivity, viscosity and density are measured using KD2 Pro thermal analyzer, viscometer and density meter respectively. The thermal conductivity values increases as the temperature and concentration increases. Whereas, the viscosity and density values decreases as the temperature increases. Cuprous oxide nanoparticles prepared by potassium hydroxide yields higher thermal conductivity values. The enhanced thermophysical properties proves that the cuprous oxide nanofluid have high potential for heat transfer applications. Hence, the objectives of the project are met.

For the future work of the project, further analysis on the thermophysical properties should be done. Other properties including specific heat of the nanofluid should be evaluated. The range of the temperatures and concentration should be increased too. Besides that, the hollow structure of the cuprous oxide nanoparticles should be further studied in detail. Besides sodium bicarbonate, other chemicals such as potassium bicarbonate and ammonium bicarbonate should be used to analyze the nucleation process of the hollow structure.

REFERENCES

- Ahmed, J., Trinh, P., Mugweru, A. M., & Ganguli, A. K. (2011). Self-assembly of copper nanoparticles (cubes, rods and spherical nanostructures): Significant role of morphology on hydrogen and oxygen evolution efficiencies. *Solid State Sciences*, *13*(5), 855–861.
- Bao, H., Zhang, W., Shang, D., Hua, Q., Ma, Y., Jiang, Z., . . . Huang, W. (2010). Shape-Dependent Reducibility of Cuprous Oxide Nanocrystals. *The Journal of Physical Chemistry C*, *114*(14), 6676–6680.
- Basu, M., Sinha, A. K., Pradhan, M., Sarkar, S., Govind, & Pal, T. (2011). CuO barrier limited corrosion of solid Cu₂O leading to preferential transport of Cu(I) ion for hollow Cu₇S₄ cube formation. *Journal of Physical Chemistry C*, *115*(25), 12275–12282.
- Cao, Y., Xu, Y., Hao, H., & Zhang, G. (2014). Room temperature additive-free synthesis of uniform Cu₂O nanocubes with tunable size from 20 nm to 500 nm and photocatalytic property. *Materials Letters*, *114*(0), 88–91.
- Ghosh, S., Roy, M., & Naskar, M. K. (2014). A Facile Soft-Chemical Synthesis of Cube-Shaped Mesoporous CuO with Microcarpet-Like Interior. *Crystal Growth & Design*, *14*(6), 2977–2984.
- Goel, P., Duragasi, G., & Singh, J. P. (2013). Copper(I) oxide micro-cubical structures formation by metal organic chemical vapor deposition from copper(II) acetylacetonate. *Journal of Materials Science*, *48*(14), 4876–4882.
- Hu, Q., Wang, F., Fang, Z., & Liu, X. (2012). Cu₂O–Au nanocomposites for enzyme-free glucose sensing with enhanced performances. *Colloids and Surfaces B: Biointerfaces*, *95*(0), 279–283.
- Hua, Q., Shang, D., Zhang, W., Chen, K., Chang, S., Ma, Y., . . . Huang, W. (2011). Morphological Evolution of Cu₂O Nanocrystals in an Acid Solution: Stability of Different Crystal Planes. *Langmuir*, *27*(2), 665–671.
- Huang, L., Peng, F., Yu, H., & Wang, H. (2008). Synthesis of Cu₂O nanoboxes, nanocubes and nanospheres by polyol process and their adsorption characteristic. *Materials Research Bulletin*, *43*(11), 3047–3053.
- Kavitha, T., Rajendran, A., Durairajan, A., & Shanmugam, A. (2012). Heat transfer enhancement using nanofluids and innovative methods - An overview.

- Kumaresan, G., Venkatachalapathy, S., & Asirvatham, L. G. (2014). Experimental investigation on enhancement in thermal characteristics of sintered wick heat pipe using CuO nanofluids. *International Journal of Heat and Mass Transfer*, 72(0), 507-516.
- Kumaresan, G., Venkatachalapathy, S., Asirvatham, L. G., & Wongwises, S. (2014). Comparative study on heat transfer characteristics of sintered and mesh wick heat pipes using CuO nanofluids. *International Communications in Heat and Mass Transfer*, 57(0), 208–215.
- Li, B., Li, Y., Zhao, Y., & Sun, L. (2013). Shape-controlled synthesis of Cu₂O nano/microcrystals and their antibacterial activity. *Journal of Physics and Chemistry of Solids*, 74(12), 1842–1847.
- Li, Y., Zhou, J. e., Tung, S., Schneider, E., & Xi, S. (2009). A review on development of nanofluid preparation and characterization. *Powder Technology*, 196(2), 89–101.
- Lin, Y.-K., Chiang, Y.-J., & Hsu, Y.-J. (2014). Metal–Cu₂O core–shell nanocrystals for gas sensing applications: Effect of metal composition. *Sensors and Actuators B: Chemical*, 204(0), 190–196.
- Ma, L.-L., Li, J.-L., Sun, H.-Z., Qiu, M.-Q., Wang, J.-B., Chen, J.-Y., & Yu, Y. (2010). Self-assembled Cu₂O flowerlike architecture: Polyol synthesis, photocatalytic activity and stability under simulated solar light. *Materials Research Bulletin*, 45(8), 961–968.
- Park, H. J., Choi, N.-J., Kang, H., Jung, M. Y., Park, J. W., Park, K. H., & Lee, D.-S. (2014). A ppb-level formaldehyde gas sensor based on CuO nanocubes prepared using a polyol process. *Sensors and Actuators B: Chemical*, 203(0), 282–288.
- Peyghambarzadeh, S. M., Hashemabadi, S. H., Naraki, M., & Vermahmoudi, Y. (2013). Experimental study of overall heat transfer coefficient in the application of dilute nanofluids in the car radiator. *Applied Thermal Engineering*, 52(1), 8–16.
- Sarafraz, M. M., & Hormozi, F. (2014). Convective boiling and particulate fouling of stabilized CuO-ethylene glycol nanofluids inside the annular heat exchanger. *International Communications in Heat and Mass Transfer*, 53(0), 116–123.
- Sekhar, H., & Narayana Rao, D. (2012). Preparation, characterization and nonlinear absorption studies of cuprous oxide nanoclusters, micro-cubes and micro-particles. *Journal of Nanoparticle Research*, 14(7), 1–11.
- Sharma, P., & Sharma, S. K. (2013). Microscopic investigations of Cu₂O nanostructures. *Journal of Alloys and Compounds*, 557(0), 152–159.
- Sundar, L. S., Farooky, M. H., Sarada, S. N., & Singh, M. K. (2013). Experimental thermal conductivity of ethylene glycol and water mixture based low volume

- concentration of Al₂O₃ and CuO nanofluids. *International Communications in Heat and Mass Transfer*, 41(0), 41–46.
- Timofeeva, E., Yu, W., France, D., Singh, D., & Routbort, J. (2011). Nanofluids for heat transfer: an engineering approach. *Nanoscale Research Letters*, 6(1), 182.
- Wu, S., Liu, T., Zeng, W., Cao, S., Pan, K., Li, S., . . . Peng, X. (2014). Octahedral cuprous oxide synthesized by hydrothermal method in ethanolamine/distilled water mixed solution. *Journal of Materials Science: Materials in Electronics*, 25(2), 974–980.
- Yu, W., & Xie, H. (2012). A Review on Nanofluids: Preparation, Stability Mechanisms, and Applications. *Journal of Nanomaterials*, 2012, 17.
- Zahmakıran, M., Özkar, S., Kodaira, T., & Shiomi, T. (2009). A novel, simple, organic free preparation and characterization of water dispersible photoluminescent Cu₂O nanocubes. *Materials Letters*, 63(3–4), 400–402.
- Zhang, Q., Zhang, K., Xu, D., Yang, G., Huang, H., Nie, F., . . . Yang, S. (2014). CuO nanostructures: Synthesis, characterization, growth mechanisms, fundamental properties, and applications. *Progress in Materials Science*, 60(0), 208–337.
- Zhao, H. Y., Wang, Y. F., & Zeng, J. H. (2008). Hydrothermal Synthesis of Uniform Cuprous Oxide Microcrystals with Controlled Morphology. *Crystal Growth & Design*, 8(10), 3731–3734.
- Zhou, L.-J., Zou, Y.-C., Zhao, J., Wang, P.-P., Feng, L.-L., Sun, L.-W., . . . Li, G.-D. (2013). Facile synthesis of highly stable and porous Cu₂O/CuO cubes with enhanced gas sensing properties. *Sensors and Actuators B: Chemical*, 188(0), 533–539.
- Zhu, J., Bi, H., Wang, Y., Wang, X., Yang, X., & Lu, L. (2008). Solution-phase synthesis of Cu₂O cubes using CuO as a precursor. *Materials Letters*, 62(14), 2081–2083.

APPENDIX

Appendix 1: Literature Review

No.	Author	Paper title	Synthesis method	Precursor	Sample preparation	Size/Shape of nanoparticle
1	Sourav Ghosh, Mouni Roy, and Milan Kanti Naskar	A Facile Soft-Chemical Synthesis of Cube-Shaped Mesoporous CuO with Microcarpet-Like Interior	Facile aqueous-based process	$\text{Cu}(\text{NO}_3)_2$	4 mmol TBC + 70 ml Millipore water + 20 mmol $\text{Cu}(\text{NO}_3)_2 \cdot 3\text{H}_2\text{O}$ + 70 ml DW + 60 mL of 12 mmol $\text{C}_2\text{H}_2\text{O}_4$ + 2 ml H_3PO_4	Cube-shape and carpet-like multi shell patterned structure of CuO
2	Park, Hyung Ju, Choi, Nak-Jin, Kang, Hyuntae, Jung, Moon Youn, Park, Jeong Won, Park, Kang Hyun, Lee, Dae-Sik	A ppb-level formaldehyde gas sensor based on CuO nanocubes prepared using a polyol process	Thermal oxidation	$\text{C}_{10}\text{H}_{16}\text{CuO}_4$	4.0 mmol of $\text{C}_{10}\text{H}_{16}\text{CuO}_4$ + 15 ml of a $\text{C}_5\text{H}_{12}\text{O}_2$ + 5.3g $(\text{C}_6\text{H}_9\text{NO})_n$	Average edge size of a cube was about 90 nm

3	Pratibha Goel, Ganesh Duragasi, J. P. Singh	Copper(I) oxide micro-cubical structures formation by metal organic chemical vapor deposition from copper(II) acetylacetonate	Chemical vapor deposition method	$\text{Cu}(\text{C}_5\text{H}_7\text{O}_2)_2$	Quartz tube (with external and internal diameters of 55 and 50 mm) + acetone cleaned p-type Si (100) and glass slides	Well-faceted micro-cube structure, edge length of about 800 nm
4	Mrinmoyee Basu, Arun Kumar Sinha, Mukul Pradhan, Sougata Sarkar, Govind, Tarasankar Pal	CuO Barrier Limited Corrosion of Solid Cu_2O Leading to Preferential Transport of Cu(I) Ion for Hollow Cu_7S_4 Cube Formation	Facile, wet chemical route	CuSO_4	10 mL of 0.01 M CuSO_4 + 10 mL of 0.01 M EDTA + 1 mL of 0.1 M $\text{C}_6\text{H}_{12}\text{O}_6$ + 1 mL of 1 M NaOH	Well-defined, uniform, solid, cubic morphology
5	Zhou, Li-Jing, Zou, Yong-Cun, Zhao, Jun, Wang, Pei-Pei, Feng, Liang-Liang, Sun, Li-Wei, Wang, De-Jun, Li, Guo- Dong	Facile synthesis of highly stable and porous $\text{Cu}_2\text{O}/\text{CuO}$ cubes with enhanced gas sensing properties	Hydro-thermal	$\text{Cu}(\text{NO}_3)_2$	2.71 g $\text{Cu}(\text{NO}_3)_2 \cdot 3\text{H}_2\text{O}$ + 50 mL deionized water (H_2O), $\text{C}_2\text{H}_6\text{O}_2$	Pore size is around 30 nm
6	He Ying Zhao, Ye Feng Wan and Jing Hui Zeng	Hydrothermal Synthesis of Uniform Cuprous Oxide Microcrystals with Controlled Morphology	Hydro-thermal method	$\text{Cu}(\text{NO}_3)_2 \cdot 3\text{H}_2\text{O}$	30 mL of 0.05-0.01 M $\text{Cu}(\text{NO}_3)_2 \cdot 3\text{H}_2\text{O}$ + 2 mL of CH_2O_2	Well-defined cubes, edge length of about 5 μm

7	H. Sekhar, D. Narayana Rao	Preparation, characterization and nonlinear absorption studies of cuprous oxide nanoclusters, micro-cubes and micro-particles	Co-precipitation method	CuSO ₄ ·5H ₂ O	2.5 g CuSO ₄ ·5H ₂ O + 20 mL milli Q water + 0.8 g, 0.5 mol L ⁻¹ NaOH + 40 ml milli Q water + 20 ml CuSO ₄ + 0.88 g C ₆ H ₈ O ₆ + 50 ml milli Q water	Size varying between 15 and 20 nm and agglomerated with 100–150 nm size
8	Yanyan Cao, Yanyan Xu n, Hongying Hao, Guoying Zhang	Room temperature additive-free synthesis of uniform Cu ₂ O nanocubes with tunable size from 20 nm to 500 nm and photocatalytic property	Facile additive-free aqueous solution route	Cu(CH ₃ COO) ₂	10.0 mL of 0.009 M C ₆ H ₈ O ₆ + 16.0 mL of 0.113 M NaOH + 16.0 mL of 0.005 M Cu(CH ₃ COO) ₂	Well-defined shape, uniform size and good dispersibility, 110–130 nm in side length
9	Junwu Zhu, Huiping Bi, Yanping Wang, Xin Wang, Xujie Yang, Lude Lu	Solution-phase synthesis of Cu ₂ O cubes using CuO as a precursor	Facile synthesis	Cu(CH ₃ COO) ₃	300 mL of 0.02M Cu(CH ₃ COO) ₃ + 1 mL C ₂ H ₄ O ₂ + 0.8 g of NaOH solid + 100 mL H ₂ O + 0.25 mL of 4 M N ₂ H ₄	Well-dispersed cubic particles with an edge length of 0.7–1.2 μm

10	Yongming Sui, Wuyou Fu, Haibin Yang Yi Zeng Yanyan Zhang Qiang Zhao Yangen Li Xiaoming ZhouYan Len Minghui Liand Guangtian Zo	Low temperature synthesis of Cu ₂ O crystals: shape evolution and growth mechanism	Reduction method	CuSO ₄ .5H ₂ O	17mL of H ₂ O + 1mL of 0.68 M CuSO ₄ .5H ₂ O + 0.3g of PVP + 0.74M of Na ₃ C ₆ H ₅ O ₇ + 1.2M of Na ₂ CO ₃ + 1ml of 1.4M of C ₆ H ₁₂ O ₆	Average edge length is measured to be about 800 nm
11	Qing Hua, Daili Shang, Wenhua Zhang, Kai Chen, Sujie Chang, Yunsheng Ma, Zhiquan Jiang Jinlong Yang and Weixin Huang	Morphological evolution of Cu ₂ O nanocrystals in an acid solution: stability of different crystal planes	N/A	CuCl ₂	5.0 mL of 2.0 mol/L NaOH + 50 mL of 0.01 mol/L CuCl ₂ + 5.0 ml of 0.6 mol/L C ₆ H ₈ O ₆	400-700 nm
12	Shufang Wu, Tianmo Liu, Wen Zeng, Shixiu Cao, Kanguan Pan, Shiyang Li, Yongsong Yan, Jiejun He, Bin Miao, Xianghe Pen	Octahedral cuprous oxide synthesized by hydrothermal method in ethanolamine/distilled water mixed solution	Hydro- thermal method	CuSO ₄ .5H ₂ O	0.45g of CuSO ₄ .5H ₂ O + 59.5 ml of distilled water + 0.1 ml of C ₂ H ₇ NO + 0.23g of NaOH + 54.9 ml of distilled water + 0.1 ml of C ₂ H ₇ NO + 0.1007 g SDS + 6.875 ml of N ₂ H ₄ H ₂ O	Edge length of about 860 nm

13	Yin-Kai Lin, Yu-Ju Chiang, Yung-Jung Hsu	Metal–Cu ₂ O core–shell nanocrystals for gas sensing applications: Effect of metal composition	Chemical reduction method	CuSO ₄	40 ml of 0.03 mmol CuSO ₄ + 0.5 ml of 1 M NaOH + 0.5 mL of 0.1 M C ₆ H ₈ O ₆	100 nm
14	Jahangeer Ahmeda, Phong Trinh b, Amos M. Mugweru b, Ashok K. Ganguli	Self-assembly of copper nanoparticles (cubes, rods and spherical nanostructures): Significant role of morphology on hydrogen and oxygen evolution efficiency	Micro emulsion method	Cu(NO ₃) ₂ ·3H ₂ O	0.1 M Cu(NO ₃) ₂ ·3H ₂ O + (microemulsions : 16.76% of CTAB, 13.90% of 1-butanol, 59.29% of isooctane and 10.05% of the aqueous phase)	50 to 100 nm
15	Huizhi Bao, Wenhua Zhang, Daili Shang, Qing Hua, Yunsheng Ma Zhiquan, Jiang Jinlong Yang, Weixin Huan	Shape-Dependent Reducibility of Cuprous Oxide Nanocrystals	N/A	CuCl ₂	5.0 mL of 2.0 mol·L ⁻¹ NaOH + 50 mL of 0.01 mol·L ⁻¹ CuCl ₂ + 5.0 mL of 0.6 mol·L ⁻¹ C ₆ H ₈ O ₆	400-700 nm
16	Qing Li, Ping Xu, Bin Zhang, Hsinhan Tsai, Shijian Zheng, Gang Wu, Hsing-Lin Wang	Structure-Dependent Electrocatalytic Properties of Cu ₂ O Nanocrystals for Oxygen Reduction Reaction	Reductive solution route	Cu(CH ₃ COO) ₂	0.5 g of PEG + 10 mL of 0.1 mM Cu(CH ₃ COO) ₂ + 50 μL of 6.0 M NaOH + 0.2 mL of 1 M C ₆ H ₈ O ₆	40 nm

17	Mehmet Zahmakıran, Saim Özkar, Tetsuya Kodaira, Toru Shiomi	A novel, simple, organic free preparation and characterization of water dispersible photoluminescent Cu ₂ O nanocubes	Reduction method	CuSO ₄ ·5H ₂ O	7.9 mg of 0.02 mmol Na ₃ PO ₄ ·12H ₂ O + 20 mL of 1 mM CuSO ₄ + 2 mL of 100 mM NaBH ₄	Mean diameter of 1.6±0.8 nm
18	Qiyang Hua, Fenyun Wang, Zhen Fang, Xiaowang Liu	Cu ₂ O–Au nanocomposites for enzyme-free glucose sensing with enhanced performances	Facile method	CuCl ₂	5.0 mL of 0.1M CuCl ₂ + 15.0 mL of 0.2M NaOH + 200 mL distilled water + 10.0-mL of 0.1M l-ascorbic acid	100nm
19	Mokhtar Ali, Naresh Kumar Rotte, Vadali V.S.S. Srikanth	Honey aided solution synthesis of polycrystalline Cu ₂ O particles	Solution synthesis process	CuCl ₂ ·2H ₂ O	3 ml of edible honey + 1.705 g of CuCl ₂ ·2H ₂ O + 2 g of NaOH + 50 ml of distilled water	Mixed morphology (spherical, pyramidal and cuboidal)
20	Poonam Sharma, Shatendra K. Sharma	Microscopic investigations of Cu ₂ O nanostructures	N/A	CuCl ₂	10 ml of 2.93M CuCl ₂ + 10 ml of 13.75M NaOH + 10 ml of 2.74M CTAB + 5ml of 2M N ₂ H ₄	500nm
21	Li-Li Maa, Jia-Lin Li, Hai-Zhen Sun, Ming-Qiang Qi, Jian-Bo Wang, Jin-Yi Chene, Ying Yu	Self-assembled Cu ₂ O flowerlike architecture: Polyol synthesis, photocatalytic activity and stability under simulated solar light	Polyol process	Cu(CH ₃ COO) ₂ ·H ₂ O	2.3 mmol of Cu(CH ₃ COO) ₂ ·H ₂ O + 50ml of DEG + 2.5ml of distilled water	100nm Thickness of less than 15 nm

22	Binjie Li, Yuanyuan Li, Yanbao Zhaon, Lei Sun	Shape-controlled synthesis of Cu ₂ O nano/microcrystals and their antibacterial activity	N/A	CuSO ₄	0.3–5.4 g of PVP + 0.15g of CuSO ₄ + 18 mL of deionized water + 2mL of 0.6M sodium citrate + 0.6M sodium carbonate + 1mL of 0.7–2.8 M glucose	Side length is ranging from 150 nm to 600 nm
23	Yueli Wena, Wei Huang, Bin Wang, Jinchuan Fana, Zhihua Gaoa, Lihua Yin	Synthesis of Cu nanoparticles for large-scale preparation	N/A	Cu(NO ₃) ₂ ·3H ₂ O	0.13 or 0.67 mol Cu(NO ₃) ₃ + 1000 mL DEA	Average edge length of 15 nm, with a standard deviation of the length of 5 nm
24	Lei Huang, Feng Peng, Hao Yu, Hongjuan Wang	Synthesis of Cu ₂ O nanoboxes, nanocubes and nanospheres by polyol process and their adsorption characteristic	Reduction method	Cu(CH ₃ COO) ₂ ·H ₂ O	0.005 mol Cu(CH ₃ COO) ₂ ·H ₂ O + 100 ml EG + 0.2 mmol PVP	Broken cubes or spheres were observed, average size of 100 nm
25	CAO Yan, WANG Yue-jun, ZHOU Kang-gen, BI Zhen	Morphology control of ultrafine cuprous oxide powder and its growth mechanism	Reduction method	CuSO ₄	1.0 mol/L CuSO ₄ + 5.0 mol/L NaOH + 2.0 mol/L glucose	1 micrometer